ADVANCES IN ATMOSPHERIC SCIENCES, VOL. 23, NO. 3, 2006, 323–341

Multi-year Simulations and Experimental Seasonal Predictions for Rainy Seasons in China by Using a Nested Regional Climate Model (RegCM_NCC). Part I: Sensitivity Study

DING Yihui*[1] (丁一汇), SHI Xueli[1] (史学丽), LIU Yiming[1] (刘一鸣), LIU Yan[2] (刘 艳), LI Qingquan[1] (李清泉), QIAN Yongfu[3] (钱永甫), MIAO Manqian[3] (苗曼倩), ZHAI Guoqing[4] (翟国庆), and GAO Kun[4] (高 昆)

[1] *Laboratory for Climate Studies, National Climate Center, China Meteorological Administration, Beijing* 100081

[2] *Chinese Academy of Meteorological Science, China Meteorological Administration, Beijing* 100081

[3] *Department of Atmospheric Sciences, Nanjing University, Nanjing* 210093

[4] *Department of Geoscience, Zhejiang University, Hangzhou* 310027

(Received 20 May 2005; revised 23 November 2005)

ABSTRACT

A modified version of the NCAR/RegCM2 has been developed at the National Climate Center (NCC), China Meteorological Administration, through a series of sensitivity experiments and multi-year simulations and hindcasts, with a special emphasis on the adequate choice of physical parameterization schemes suitable for the East Asian monsoon climate. This regional climate model is nested with the NCC/IAP (Institute of Atmospheric Physics) T63 coupled GCM to make an experimental seasonal prediction for China and East Asia. The four-year (2001 to 2004) prediction results are encouraging. This paper is the first part of a two-part paper, and it mainly describes the sensitivity study of the physical process parameterization represented in the model. The systematic errors produced by the different physical parameterization schemes such as the land surface processes, convective precipitation, cloud-radiation transfer process, boundary layer process and large-scale terrain features have been identified based on multi-year and extreme flooding event simulations. A number of comparative experiments has shown that the mass flux scheme (MFS) and Betts-Miller scheme (BM) for convective precipitation, the LPMI (land surface process model I) and LPMII (land surface process model II) for the land surface process, the CCM3 radiation transfer scheme for cloud-radiation transfer processes, the TKE (turbulent kinetic energy) scheme for the boundary layer processes and the topography treatment schemes for the Tibetan Plateau are suitable for simulations and prediction of the East Asia monsoon climate in rainy seasons. Based on the above sensitivity study, a modified version of the RegCM2 (RegCM_NCC) has been set up for climate simulations and seasonal predictions.

Key words: regional climate model, sensitivity experiment, physical process parameterization, mei-yu

doi: 10.1007/s00376-006-0323-8

1. Introduction

In the last decade, regional climate models have been mainly used in three aspects of climate research (Wang et al., 2004): (1) providing more detailed regional climate change scenarios in the late decades of the 21st century for the impact community, as a dynamical downscaling technique. Giorgi and Hewitson (2001) have made a comprehensive review and assessment of this issue. They have shown that regional climate models consistently improve the spatial detail of simulated and projected climate compared to GCMs that drive regional climate models; (2) simulations of current climate conditions, with multi-year or multi-seasonal integrations of regional climate models driven by observed (or perfect) or GCM boundary conditions. This kind of simulation not only serves to provide meaningful climate statistics, but also to evaluate the performance of regional climate models, including identifying systematic model errors and uncer-

*E-mail: dingyh@cma.gov.cn

tainties. Many investigators have simulated the current climate for different regions, seasons and durations (Giorgi and Hewitson, 2001). Steady improvements of the model climatology produced by regional climate models have been made during the past ten years. Current regional climate models can reproduce observed regional climatology with errors generally below 2°C for surface air temperature and within 5% to 50% of observed precipitation (Giorgi and Shields, 1999; Small et al., 1999; Lee and Suh, 2000). Another aspect of simulating current climate is to examine the climate variability on the different timescales. A number of investigators have studied intraseasonal, annual and interannual variability in different regional climate models. Generally, these variabilities, in particular the interannual variability can be well reproduced in sign and magnitude in regional climate models (Giorgi and Hewitson, 2001); and (3) simulation of anomalous climate episodes and extreme climate events, especially droughts and floods in different regions. Giorgi et al. (1996) conducted regional model experiments for the drought period of May–June–July (MJJ) 1988 and the flood period of MJJ 1993 in different regions of the U.S.A. Overall, the model performs reasonably in simulating various characteristics of surface climatology over the region during these two extreme periods, with total simulated precipitation being close to the observed in MJJ 1988 and lower than the observed by about 25% in MJJ 1993. Pan et al. (1995) pointed out that during the drought conditions of 1988, the relative contribution to the water cycle by local evapotranspiration is not as important as that during the flood conditions of 1993. Over East Asia, numerous studies using regional climate models have contributed to simulations of anomalous monsoon years and extreme climate events. For instance, Liu et al. (1994) simulated the summer monsoon season of 1990, which had a particularly intense monsoonal circulation. Hong et al. (1999), using the National Centers for Environmental Prediction (NCEP) regional spectral model (NCEP RSM), studied the eastern Asian monsoon activities and associated climate conditions for July 1987 and 1988, which correspond to an El Niño and a La Niña year, respectively. For the above two studies, the model results are satisfactory in terms of the simulated large-scale features.

A number of investigators have studied two extreme flooding events during the East-Asian mei-yu/Baiu seasons in 1991 and 1998. The 1991 flooding event was caused by prolonged, excessively heavy rainfalls over the middle and lower Yangtze River and Huaihe River basins which consisted of three intense precipitation episodes during two months from mid May to mid July, with total rainfall amounts of 500–800 mm recorded over the extensive areas in these two river basins (Ding, 1993). The 1998 flooding event is in many ways similar to the 1991 event, but with much greater rainfall amount and more extensive affected areas. The prolonged and excessively heavy rainfalls nearly lasted two and a half months from 11 June to the end of August along the entire Yangtze River basin, with a short break of rainfall during the period of 3–16 July. Total rainfall amounts of 700–900 mm were recorded over the extensive areas, with some regions having rainfall amounts exceeding 1000 mm (National Climate Center, 1998). The long term variation of the Asian summer monsoon in the Yangtze River regions is a major cause for this unprecedented heavy rain/flooding event (Ding and Liu, 2001). It is very difficult for GCMs to simulate well the mei-yu rain band in terms of climatology or case studies. According to Kang et al. (2002), many GCMs cannot realistically reproduce the observed mei-yu band in the region from the East China Sea to the central Pacific. Due to their extremely high rainfall amounts, complex multi-scale interactions and very prolonged durations, the simulation of these two extreme precipitation events in the East Asian monsoon regions provides an excellent opportunity for testing the performance of regional climate models. The 1991 flooding event has been simulated by many researchers (e.g., Liu et al., 1996; Ding et al., 1998; Leung et al., 1999; Wang et al., 2000; Liu and Ding, 2002a; and Luo et al., 2002). Liu and Ding (2002b) and Wang et al. (2003) have recently simulated the 1998 flooding event. Their results are encouraging, with the seasonal march of the major rain belt, associated large-scale circulations, precipitation evolution and patterns, rainfall intensity and peaks, and intraseasonal oscillations modulating the precipitation episodes reproduced to varying degrees.

In recent years, the regional climate simulations of the East Asian monsoon region have been obviously focused on by many investigators. One reason is to improve the dynamic seasonal and interannual prediction, especially the predictions of droughts and floods. Prediction skills for the seasonal rain belts in East Asia made by AGCMs (atmospheric general circulation models) or coupled GCMs are generally low, with an even lower skill for predictions of the interannual variability of precipitation (Gates et al., 1999; Sperber et al., 2001). Therefore, there is much need in the use of high resolution regional climate models to enhance the predictive capability for this region with added information. Another reason for concern about the use of regional climate models in the East Asian region is to study the unique climate conditions and variability in this part of the world (Ding, 1994). Numerous investigators have evaluated the performance of regional climate models for simulations of the East Asian climatology and extreme climate events. The major results may be summarized as follows: (1) Large-scale

features associated with the East Asian summer monsoon system and the evolutive processes of the onset, break phase and abrupt jumps between two adjacent phases of the East Asian summer monsoon are well simulated (Lee and Suh, 2000). (2) The regional climate models have fairly well reproduced the march of the major seasonal rain belts (the mei-yu in China, Baiu in Japan and Changma in Korea), including their occurrence, duration and annual and monthly rainfall patterns. (3) The large-scale circulation, evolutive processes, timing and location, rainfall amount and intraseasonal oscillations of the severe and prolonged drought and flood events can be relatively realistically simulated. However, there are a number of biases and deficiencies: (1) In the model climatology, the intensity and magnitude of large-scale features are not well reproduced (Lee and Suh, 2000;). (2) The timings of onset and ending, and the rainfall amounts of the seasonal rainy belts as well as extreme flooding events, have a considerable bias (Hong et al., 1999). Most studies have overestimated the precipitation with different departure percentages (Liu et al., 1996; Lee and Suh, 2000; Giorgi et al., 1999; Liu and Ding, 2002a, b). In contrast, some regional simulations have produced underestimated rainfall amounts (Liu et al., 1994; Wang et al., 2000; Wang et al., 2003). (3) The simulated surface air temperature generally shows a cold bias (Giorgi and Mearns, 1999; Leung et al., 1999; Wang et al., 2003). The model atmosphere is colder and drier than the observed one (Hong et al., 1999; Wang et al., 2000). (4) Very few studies have contributed to simulations of diurnal cycles (Hong et al., 1999; Leung et al., 1999). The simulated diurnal variations of precipitation and temperature show a significant deviation from the observed ones, especially for local minimums and maximums. There is a tendency to overestimate surface solar radiation and cloudiness.

Numerous investigators have made attempts to interprete these systematic biases and uncertainties in terms of different treatments of integration, lateral boundary conditions, size of domains, horizontal and vertical resolutions and different parameterization schemes of physical processes used in regional climate models (e.g., Liu et al., 2002; Pan et al., 1999; Zheng et al., 2002). Among them, four major factors in determining model performance have been identified based on various sensitivity experiments. The cloud-radiative process is very important for long-term climate simulation (Leung et al., 1999). It has serious implications for simulating the energy and hydrological cycles, especially over cloudy areas. Giorgi et al. (1999) also stressed that different formulations of large-scale cloud-producing mechanisms are shown to significantly affect cloud profiles, radiation budgets at the surface and top of the atmosphere, and as a consequence, the simulated surface climatology. The second factor is the land surface process. Variations in surface characteristics affect temperature and precipitation simulations in different ways during cold/dry and warm/wet seasons. Therefore, a reasonable vegetation-soil scheme is highly required in regional climate models. The third factor is the cloud (convective and non-convective) parameterization schemes which not only determine the simulated precipitation amounts and patterns, but also affect the cloud-radiative process through producing different horizontal and vertical distributions of clouds. Although there are a number of options for different cloud parameterization schemes, no intercomparision study can elucidate their suitability for different seasons, regions and climate conditions. The fourth factor is the inclusion of the Tibetan Plateau. Most of the present simulation domains have their western boundary located at 90°–100°E, which passes through the eastern periphery of the Tibetan Plateau. In doing so, the effects of both dynamical and thermal forcings are not properly considered (Wang et al., 2000), especially their effects on the East Asian monsoon circulation and the rain-producing weather systems originating in the Tibetan Plateau and moving eastward along the Yangtze River basin. Furthermore, differences in the representation of surface topography between the large-scale and regional models can produce gravity inertia waves that propagate to the interior of the domain, so that regional simulations can be seriously affected (Leung et al., 1999). Therefore, it is difficult to avoid placing the western boundary away from the huge Tibetan Plateau or partially including it.

Our aim is to develop a nested regional climate system which has a potential use in the seasonal prediction in China as well as in the East Asian monsoon region based on the NCC/IAP T63 coupled GCM and RegCM2 (Giorgi et al., 1993a, b; Ding et al., 2000; Ding et al., 2002; Ding et al., 2004a). To achieve this objective, a nested regional climate model (RegCM_NCC) （Ding et al., 2004b; Chan et al., 2004） has been developed with a special emphasis on the use of reasonable physical parameterization schemes and appropriate treatment of the large-scale terrain features in the East Asian region based on a series of sensitivity experiments of precipitation and temperature in China to land surface process schemes, cloud-radiative schemes, cumulus parameterization schemes and planetary boundary layer schemes as well as treatment schemes of the Tibetan Plateau. Major results of these sensitivity experiments are included in Part I of the present paper. The second part will deal with a 10-yr climate simulation in China under forcing of the NCEP reanalysis data. The model climatology in China will be discussed as compared to observed datasets to identify major biases. Then, the results of a 10-yr hindcast with the nested regional

Table 1. The design of sensitivity experiments for the main physical processes.

Physical process	RegCM2's original parameterization	Other schemes for sensitivity experiments
Land surface process	BATS (Dickinson et al., 1993)	1. Improved algorithm of exchange coefficients
		2. Improved surface process schemes: LPMI and LPMII
Convective precipitation	1. Kuo scheme (Anthes, 1977; Anthes et al., 1987)	1. Mass flux scheme (MFS)
	2. Grell scheme (Grell, 1993)	2. Betts-Miller scheme (BM)
Radiation transfer	CCM2 scheme	CCM3 scheme
Boundary layer physics	1. Nonlocal scheme of Troen and Mahrt	1. Mellor-Yamada scheme
	2. Holtslag scheme (Holtslag et al., 1990)	2. Modified TKE scheme
Large-scale topography	No specific treatment	1. Gravity wave drag
		2. Envelope topography
		3. Error reduction of horizontal pressure gradient force

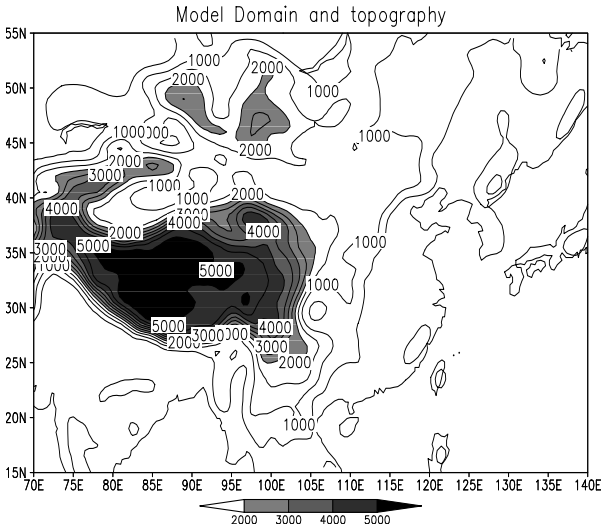

Fig. 1. The domain under study, with topographical elevation isolines.

climate model driven by NCC/IAP T63 CGCM will be discussed. The skill of the seasonal prediction for 1991/2000 will be assessed. Finally, the four-year (2001–2004) real time experimental seasonal predictions for the rainy season (June, July and August) in China will be reported.

2. Experiment design and data

The regional climate model used here for the sensitivity study is the RegCM2 (Giorgi et al., 1993a, b). In this model, the main physical processes include the land surface processes, the radiative transfer process, the large-scale and convective precipitation, and the boundary layer processes. The focus of the simulation experiments carried out in this work is placed on the sensitivity experiments of precipitation and temperature to major physical processes and large-scale topography in the domain. Table 1 is a brief summary of the design of the sensitivity experiments. The details of the sensitivity experiments for each physical process will be elaborated upon in the respective sections.

Figure 1 shows the experiment domain. The large-scale terrain features, especially the Tibetan Plateau, are included, with peak elevations of about 5000 m entirely placed within the domain. The grid horizontal resolution is 60 km.

The 160-stations dataset in China is used for validation of the simulation results. The data in the western part of China are relatively sparse, but this situation will not seriously affect our test of the simulations, because in most cases our major concern is placed on the monsoon region in East China. The NCEP and Global Energy and Water Cycle Experiment (GEWEX) reanalysis datasets were used for providing observed boundary conditions. The radiation datasets of Earth Radiation Budget Experiment (ERBE) and total cloud cover data of International Satellite Cloud Climatology Project (ISCCP) were used in this study.

3. Land surface process

The Biosphere-Atmosphere Transfer Scheme (BATS) in the regional climate model RegCM2 has one vegetation layer, one snow cover layer and three soil layers with depths of 0.1 m, 1.0–2.0 m and 10 m, respectively. According to our analysis of the multi-year and multi-layer monthly mean soil temperature data over China, it can be found that the vertical configuration of the soil temperature shows obvious seasonal and interannual variations as well as regional differences. The plant root zone (0.5–2.0 m) seems to be a transition layer between the surface layer with quick variation and the deep layer with slow variation. By using the 10-layer soil moisture station data of 1981–2000 in China, Zhang et al. (2004) also found a layer of abrupt change of soil moisture between 30 cm

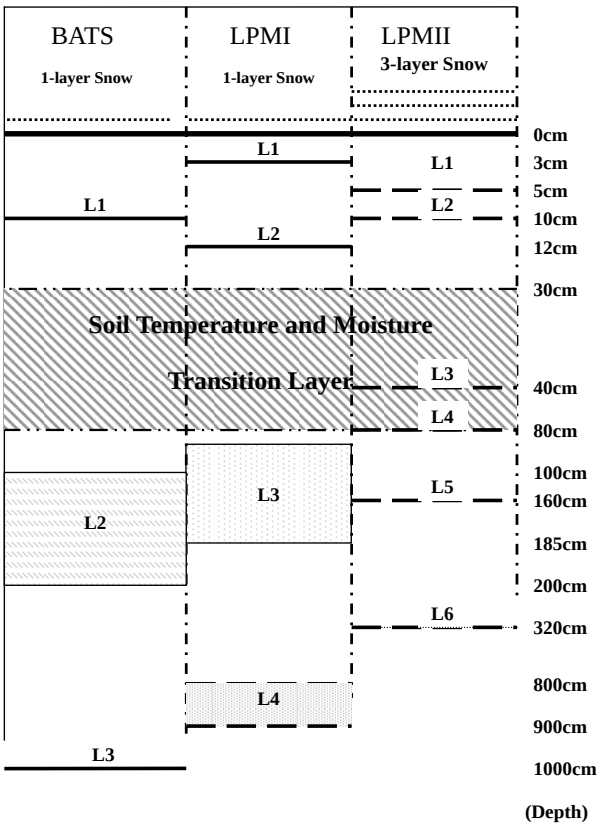

Fig. 2. Schematic diagram of the three land-surface process models.

and 80 cm, corresponding to the plant root zone layer. So, the vertical division of the soil layer in land surface models should not be too coarse, otherwise the vertical variation of soil temperature and moisture cannot be described in a realistic manner. In particular, the transition layer between the upper and deep soil layers should be described with a higher resolution. Additionally, a coarse vertical resolution will affect the calculation accuracy due to truncation error, which will further affect the simulation of various fluxes at the interface of the atmosphere and land surface.

Besides the soil vertical resolution problem, there are also some other weakness in the BATS, such as the solution method of soil temperature and moisture. The force-restore (F-R) method and some empirical relations are used in the BATS for solving soil temperature and moisture without any accurate and explicit descriptions of soil temperature conduction or soil moisture diffusion processes. It has been proved that a serious problem will arise when the F-R method is used in uneven soil and in soil with snow cover above it. In addition, the snow cover is also rather simply represented in the BATS. Except for the snow-surface process, there is no explicit distinction between subsurface snow and the underlying soil. Significant errors possibly occur during the periods of snow melting or rainfall on a snow-pack. This situation usually occurs in regions of snow cover or permanent ice over highlands such as the Tibetan Plateau. So, it is also necessary to improve the description of the snow-cover process in models to obtain better model performance. For this purpose, we have mainly modified the soil part of the BATS with two new versions (the LPMI and LPMII, see Fig. 2).

3.1 *The LPMI*

The LPMI adds one soil layer to the upper layer compared with the BATS, so the depth of each layer is 0.03 m, 0.12 m, 0.85–1.85 m and 8–9 m, respectively. The first layer is made as thin as possible to be able to express the variation of the surface, the depth of the third layer is well placed in the root zone layer, corresponding to the layer of seasonal variation, and the fourth layer represents the deep soil layer. In addition, the combination of the physical equations and empirical analytical formulae are used to construct the governing equations of soil temperature and moisture. In fact, a higher resolution of model level and physical equations are adopted for the upper soil layers, and for the deeper soil layers, a lower resolution of model level and empirical analytical formulae are used. Besides the modification of the soil process, the sub-grid distribution of rainfall and its effects are taken into account for the land surface hydrological process, and a simple snow cover model is also used to include effects of snow cover on soil thermodynamics and hydrology (Zhang and Ding, 1998).

3.2 *The LPMII*

Though an additional surface layer near the surface has been added in the LPMI, no modification has been made to the representation of the root zone layer. And from the analysis of the observed soil temperature and moisture discussed above, the deepest soil layer of 3–4 m should be sufficient if our focus is placed on the short-term climate. We have further increased the vertical resolution in the LPMII, separating the soil layer into six layers, with depths of 0.05 m, 0.01 m, 0.40 m, 0.80 m, 1.60 m and 3.20 m, respectively. Among them, the first two layers correspond to the surface layer of diurnal variation, the third and fourth layers correspond to the root zone layer, and the last two layers represent the deep soil layers. From the schematic diagram of the three models (Fig. 2), one can see that the depth of the deepest soil layer is most reduced in the LPMII and deepest in the BATS. For the layers above the root zone, the number of layers is most fine in LPMII, with five layers above 2m, while the LPMI has three layers and the BATS only two. So, the LPMII has the highest vertical resolution of soil layers among them, with two layers to describe the plant root zone.

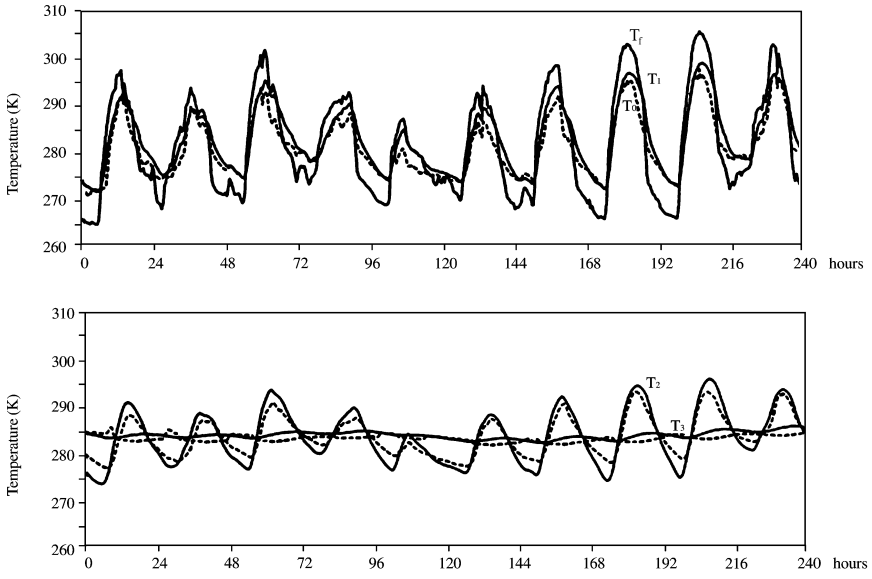

Fig. 3. The simulation results at the Zhangye site on 1–10 May 1991 based on HEIFE land process experiment data. (a) The simulated (T_1) and observed (T_0) surface soil temperature and the canopy temperature (T_f), (b) the simulated and observed temperature of the second soil layer (T_2) and the third soil layer (T_3) (the simulated surface temperature is for 1.5 cm and the observed one is at the surface, the simulated second one is for 9 cm and the observed one is for 5 cm, the simulated third soil temperature is for 40 cm and the observed one is for 57.5 cm, and the simulated is a solid line, the observed is a dashed line). (Zhang and Ding, 1998).

Additionally, with the improvement of computer resources, we have also improved the solving method of soil temperature and moisture by applying the direct solution of the physical equations of soil water and energy. We also used a complex multi-layer snow submodel, which includes the destruction processes and estimates of energy and water exchange in the snow cover.

3.3 *Sensitivity experiments with the LPMI and LPMII*

First, a series of "offline" experiments have been made to verify the performance of the LPMs. Fig. 3 shows some results of the offline experiments with LPMI based on the data of the Zhangye station (38.9°N, 100.6°E) covered with crops during the HEIFE land process field experiments. It can be seen that the simulated and observed temperatures for each soil layer are generally consistent. Because the simulated and observed temperatures are not exactly at the same depths of the soil, there is a little difference between the simulated and observed variations. The offline experiment of the LPMII with the GEWEX/GAME/HUBEX experiment data has been undertaken, with the variation of soil temperature reasonably captured (figure not shown).

The LPMI and LPMII have also been respectively coupled with the RegCM2 as an option other than BATS to describe the land surface process. The excessively heavy rainfall process in summer 1991 over the Yangtze River-Huaihe River Basins has been selected as a case study to test the performance of the regional climate model coupled with three land-surface process models. The major differences are reflected in simulations of the surface temperature (Fig. 4). The BATS simulated a very high unrealistic surface temperature in the southern part of the domain (Fig. 4b) where the surface temperatures simulated with the LPMI and LPMII (Figs. 4c and d) have been effectively reduced, though they are still somewhat higher than the observations. The precipitation simulations with the LPMI and LPMII were also improved, mainly with the location of the precipitation maximum shifted to the land area (the lower basin of the Yangtze River-Huaihe River) and the rain amount enhanced (figure not shown). So, the simulations of land surface variables can be effectively improved after modifying the soil vertical resolution and the solving method for soil temperature and moisture.

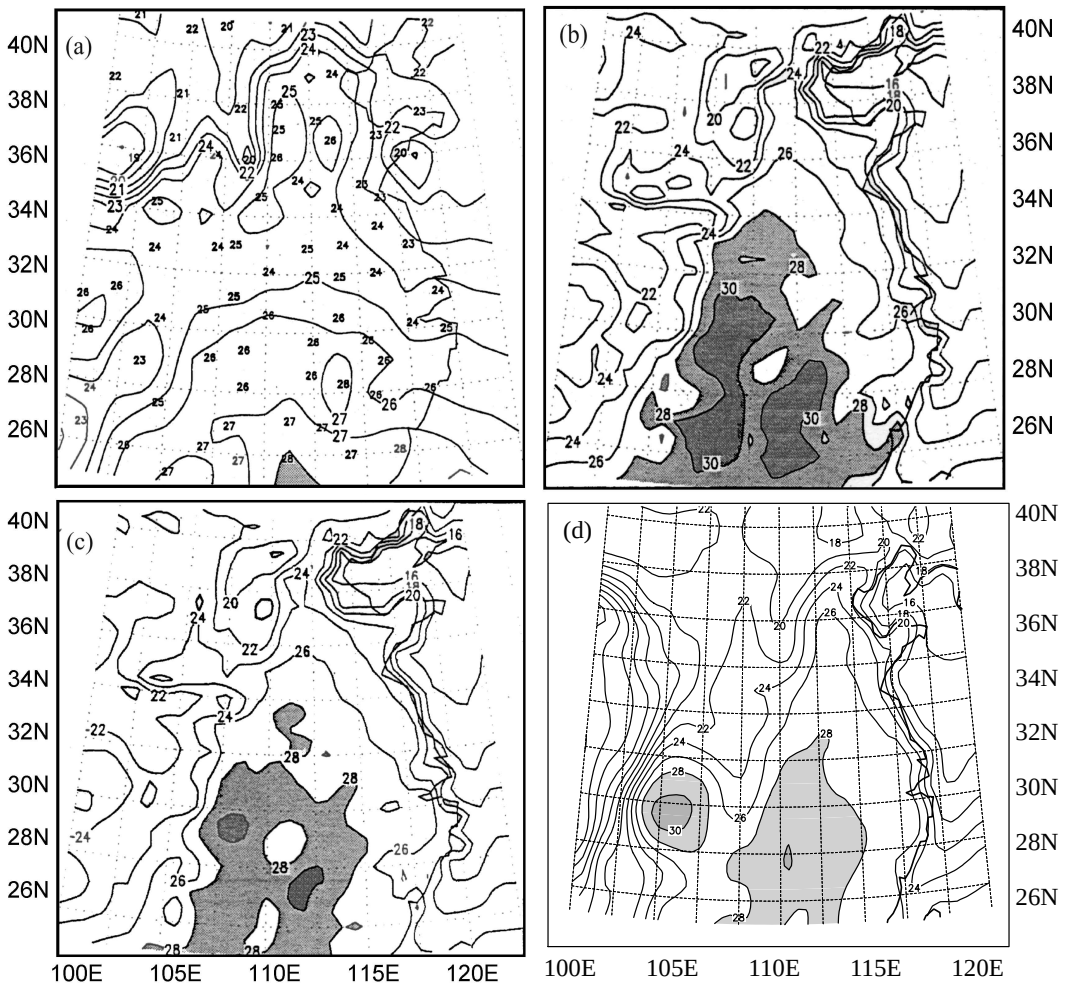

Fig. 4. Monthly mean surface air temperature of June 1991 (Unit: °C). (a) Observation, (b) simulation with BATS, (c) simulation with LPMI and (d) simulation with LPMII. (Partly from Ding et al., 1998).

4. Convective precipitation process

The convective precipitation is highly sensitive to the cumulus parameterization schemes. Two major problems with convective precipitation exist in the RegCM2, which uses the Kuo scheme and Grell scheme for this purpose. One problem is that a too dry regional climate is simulated with the Kuo scheme. This deficiency was expected to be eliminated or at least reduced by using the Grell scheme, an Arakawa type convective scheme, because the latter can produce more rainfall than the Kuo scheme (Liu et al., 1996). However, an intercomparision study showed that the Grell scheme still produced excessively small amounts of convective precipitation during the monsoon season over East Asia (Leung et al., 1999). Therefore, an effort to further enhance the simulated convective precipitation in this monsoon region was made by Liu and Ding (2002a) and recently by Wang et al. (2003) with the use of mass flux schemes or the Betts-Miller scheme. The second problem with the cumulus parameterization schemes in the RegCM2 is the fraction of convective to total rainfall amount. Use of the Kuo cumulus scheme resulted in a higher fraction of convective precipitation as opposed to the use of the Grell scheme. But, we will not discuss this problem here.

The MFS developed by Liu and Ding is based on the modified ECMWF mass flux cumulus scheme (Chen, 1996) and the comprehensive mass flux scheme of Tiedtke (1989). In the MFS, not only is the large-scale moisture convergence taken into account, but also the cumulus updrafts and downdrafts, cumulus-induced subsidence in the environmental air, entrainment, detrainment, and evaporation. The interaction between the cumulus and environment is described by using a one-dimensional cloud model. At the same time, this scheme includes penetrative and shallow convections. The MFS has been successfully incorporated into the RegCM2 and applied to simulate the 1991 and 1998 summer monsoon activities and heavy

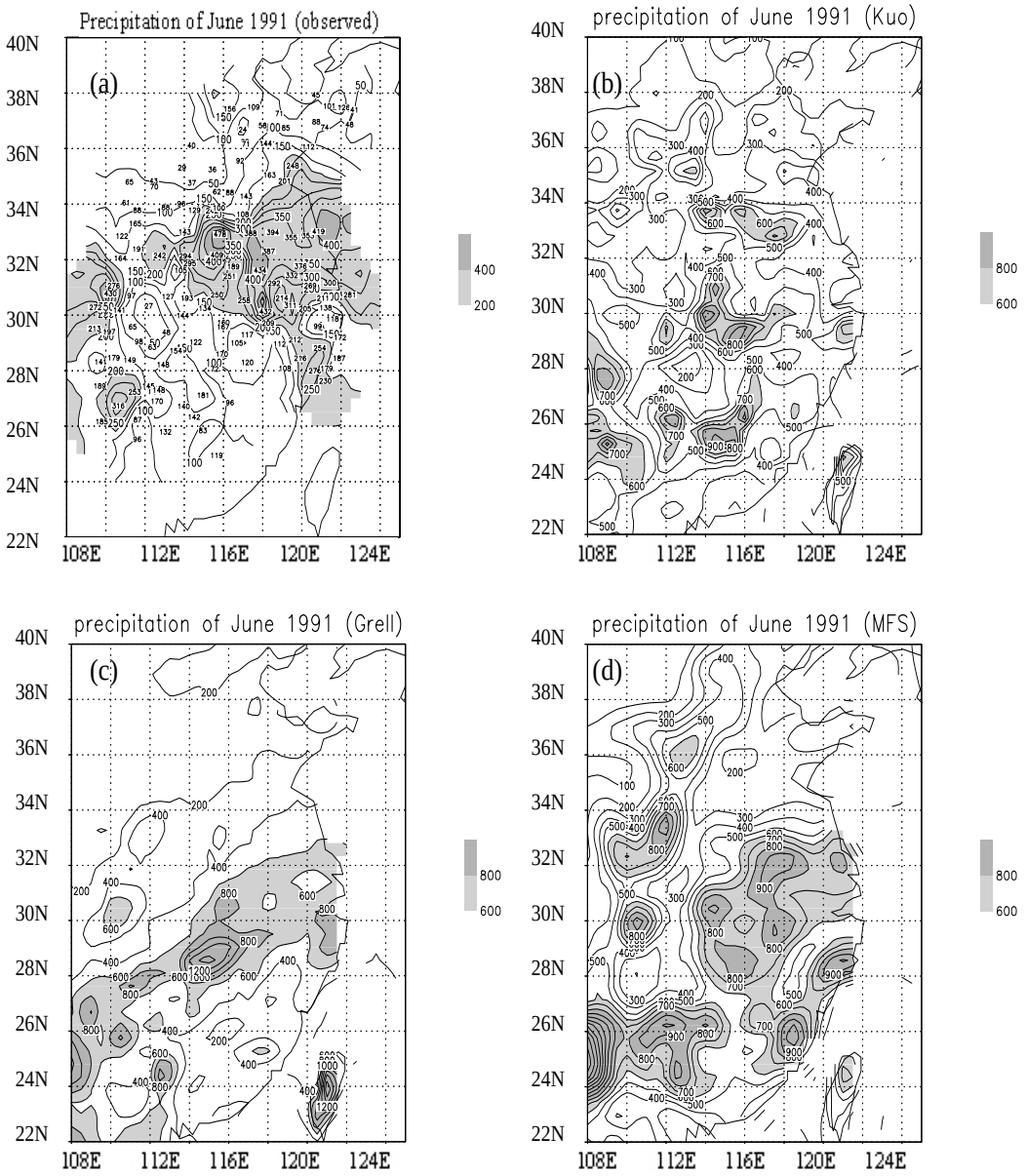

Fig. 5. The monthly precipitation patterns for June 1991 for (a) the observation, (b) simulated with the Kuo scheme, (c) the Grell scheme, and(d) simulated with the MFS scheme. Unit: mm. The precipitation exceeding 600 mm in (b)–(d) are shaded.

rainfall processes. The results show that the MFS has successfully simulated these prolonged, extreme rainfall events. With an intercomparison among the Kuo scheme, the Grell scheme and the MFS scheme, it is found that the MFS scheme has a better performance in simulating rainfall location and amount, and rain duration as well as the surface temperature. In particular, the amounts of convective precipitation were significantly enhanced. Fig. 5 is exemplified to illustrate the simulated monthly precipitation amounts in the flood region for June 1991 by the Kuo, Grell and MFS schemes. An intercomparison among them indicates that the MFS scheme simulated a more realistic precipitation pattern, with the major rainfall maxima consistent with the observed ones. But, the total rainfall amount was overestimated by the MFS scheme. The daily observed and simulated precipitations averaged over the middle and lower Yangtze River-Huaihe River basins are shown in Fig. 6. As illustrated in the introduction, the 1991 mei-yu event consists of three major episodes of excessively heavy rain episodes during the period from May to July (18–26 May, 2–19

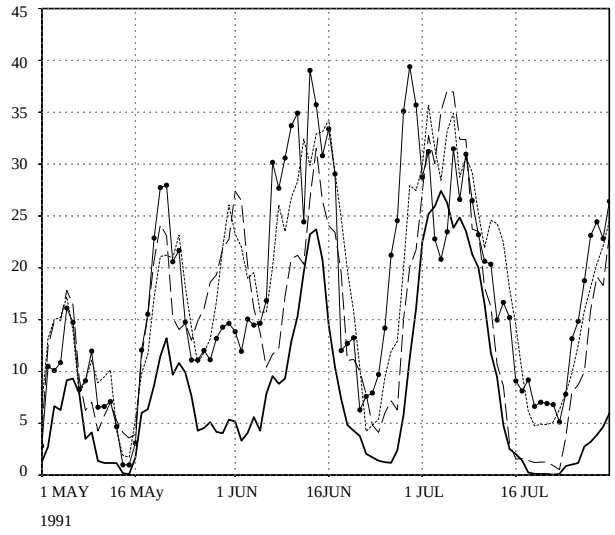

Fig. 6. Daily precipitation variations averaged over the middle and lower Yangtze River-Huaihe River basins for May–July 1991. A 5-day running average was applied to the daily curves. The bold line is the observation, the dashed line precipitation simulated with the Kuo scheme, the dotted line for the Grell scheme and the solid line with dots for the MFS. Unit: mm d^{-1}.

June, 30 June–13 July). Overall, the three cumulus parameterization schemes can simulate the day-to-day variations of daily precipitation, but with a greater daily rainfall amount than the observations. Note that the Kuo and Grell schemes simulated an unrealistic rainfall episode (27 May–1 June) between the first and the second episodes. Only the simulation with the MFS scheme correctly reproduced the three rain episodes and two breaks in between, which reflected the modulation of the rainfall period from May to July by the 20–25 day intraseasonal oscillation. Other than the precipitation simulations for the 1991 and 1998 severe flooding events, the simulation with the MFS scheme further shows a more realistic large-scale circulation, moisture transport, and atmospheric heating fields and their variations (figures not shown).

The Betts-Miller cumulus parameterization scheme (BM) was tested by using various datasets (Betts and Miller, 1986) and generally showed a good capability to simulate convective precipitation processes. In a comparative study of the Kuo, Grell and BM schemes for simulations of the 1991 and 1994 rainy seasons in East China (Ding et al., 1998), the BM scheme has a higher skill for rainfall episodes greater than 25 mm than the other schemes. For the rainfall episodes of 50 mm and 100 mm, the simulations with the BM scheme showed a more realistic pattern. Therefore, the BM scheme can be used to improve simulations of intense rainfall episodes during the rainy season in the East Asian monsoon region. The BM scheme takes into account the effects of deep convection and shallow convection, separately. It is a convection adjustment type scheme. The parameters in this scheme may be independently adjustable, through a comparison with the observed data. A sensitivity test has been recently made for verification of the adjustable parameters such as adjustment timescale, stability parameter and saturation pressure departure at the cloud base and freezing level. The results have shown that the regional precipitation patterns and amounts during flooding seasons in East China are rather sensitive to them. Based on the sensitivity tests, an optimal parameter set of the BM scheme is derived. This scheme was used in the RegCM2 to simulate the climate of the 1991 and 1994 flooding seasons. The observed and simulated precipitation patterns for the 1991 flooding season (1 May–15 July) are in good agreement in the locations of the rainfall maximum and the total rainfall amounts (Zhai et al., 2003). The observed and simulated pentad-to-pentad precipitation variations also indicated the same three rainfall episodes (figure not shown), both with lower simulated rainfall amount for the second and third episode than the observed, but with a better correspondence to the observed one than the other schemes. Based on the above sensitivity experiments, the MFS and BM schemes can be separately used in the RegCM2 to produce the model climatology and seasonal predictions.

5. Cloud-radiation process

Cloud-radiation interaction is one of the most important physical processes in East Asian monsoon climate. Using three regional models to simulate the 1991 summer extreme flood events, Leung et al. (1999) concluded that many significant problems would arise, especially the simulated energy and hydrological cycles over cloudy areas, due to the uncertainties of the cloud-radiation transfer process. So more attention should be paid to the cloud-radiation process in regional climate models. Thereafter, Giorgi et al. (1999) also pointed out that the representation of the cloud-radiation process was rather crude in the RegCM2, which had been so far largely neglected and was clearly in need of improvement.

Based on the 5-year continuous simulations of present day climate (1997–2001), firstly we validated the performance of the CCM3 cloud-radiation parameterization scheme for use in the regional climate simulation over China. The general description of the CCM3 radiation transfer scheme may be found in Kiehl et al. (1996). The model domain is from 70° to 145°E and from 10° to 55°N, with a 60-km horizon-

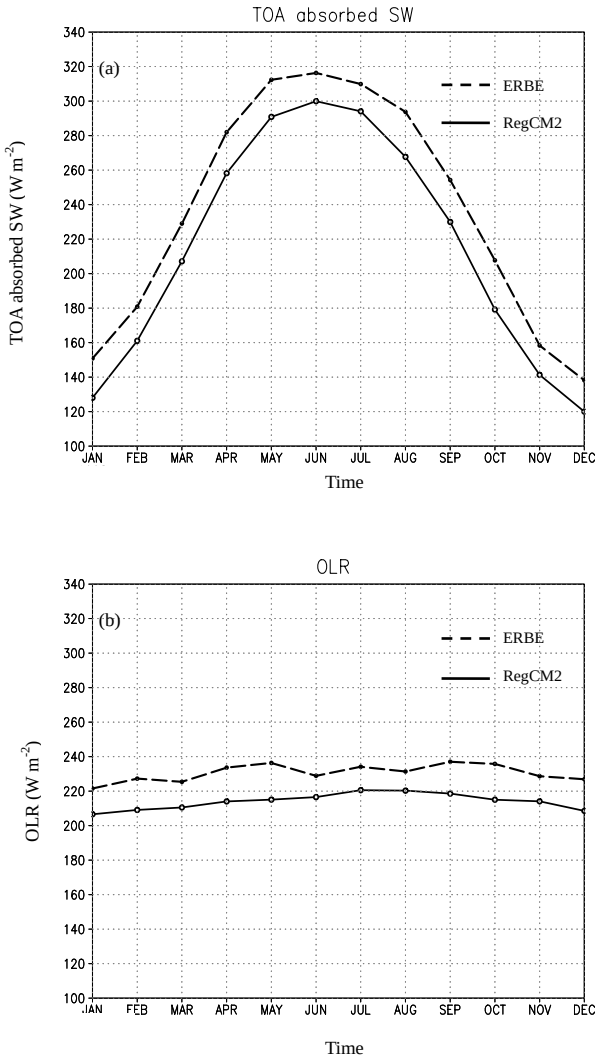

Fig. 7. The annual variations of (a) the absorbed shortwave radiation (SW) and (b) the outgoing longwave radiation (OLR) at the top of the atmosphere (TOA).

tal resolution and 14 vertical levels. Then, with the purpose of testing some key parameters of the scheme, a series of sensitivity experiments were carried out, focusing on the weaknesses and strengths in the simulations of the climate characteristics of China. The data used to verify the model are ERBE (Barkstrom, 1984) and ISCCP (Rossow and Schiffer, 1991) data with $2.5^\circ \times 2.5^\circ$ resolution. Due to the different resolutions between the satellite data and model output, the satellite data were interpolated into the model grid firstly in order for them to be compared. At the same time, it is noted that the monthly and annual mean ERBE data are averaged from 1985 to 1989, and the ISCCP data are from 1984 to 1988, while the RegCM2 outputs are averaged from 1997 to 2001. The reliability of the comparison might be weakened somewhat because of the inconsistency of the time intervals. However, this will not affect the validations of the model performance and system bias so much, because we mainly study the climatological characteristics of the radiation and cloud fields.

Figure 7 is the seasonal variations of annual mean TOA (top of the atmosphere) absorbed shortwave radiation (SW) flux and the outgoing longwave radiation (OLR) flux over China. One can see that the seasonal variation of each radiation component can be simulated well, except for some differences in magnitude. The simulated TOA SW and OLR are consistently 20 W m^{-2} and 15 W m^{-2} lower than the observed ones, respectively, so the net radiation budget at TOA has a negative bias of 5.65 W m^{-2} (Table 2). This would lead to a cold bias for the model climatology. The simulated geographical distributions of the TOA SW and OLR flux compare well with the satellite observations. However, two major bias regions of the simulated TOA absorbed SW radiation are found in the Yangtze River-Huaihe River Basins and the Tibetan Plateau (Fig. 8a). The TOA absorbed SW bias pattern is consistent with that of the total cloud cover bias shown in Fig. 8b, with the reduced (increased) cloud cover corresponding to the increased (reduced) TOA absorbed SW radiation. In the Yangtze River-Huaihe River Basins, the positive TOA absorbed SW bias is likely to be contributed mainly from the negative bias of the total cloud cover, e.g., with the significantly underestimated cloud cover leading to more TOA absorbed SW radiation. In contrast, over the Tibetan Plateau, the cloud cover bias is only 10%–20% higher than the observations, while the TOA absorbed SW bias is much larger than those of other areas. This significant difference cannot be fully explained with the cloud cover bias. One possible reason is due to the effect of cloud optical properties. It is well known that cloud affects radiation transfer by its scattering and absorption. The calculation of SW radiation is also very sensitive to the cloud optical properties besides the cloud cover. The smaller the cloud droplet radius is, the more solar radiation is reflected. In the radiative parameterization of the RegCM2, the optical properties of the cloud droplets are represented in terms of the prognostic cloud water path and effective radius. There is a possibility that the expression of the effective radius is not fully suitable for the Tibetan Plateau areas. Presumably, the cloud droplet effective radius is relatively large in the less polluted regions, such as in the highlands in Western China. In order to further clarify the effect of the effective radius on the TOA absorbed SW flux, we use the radius value of 10 μm (a value equivalent to the cloud droplet effective radius over the sea) to replace the original effective radius to perform a sensitivity experiment, thus we find that the results can be improved obviously, which

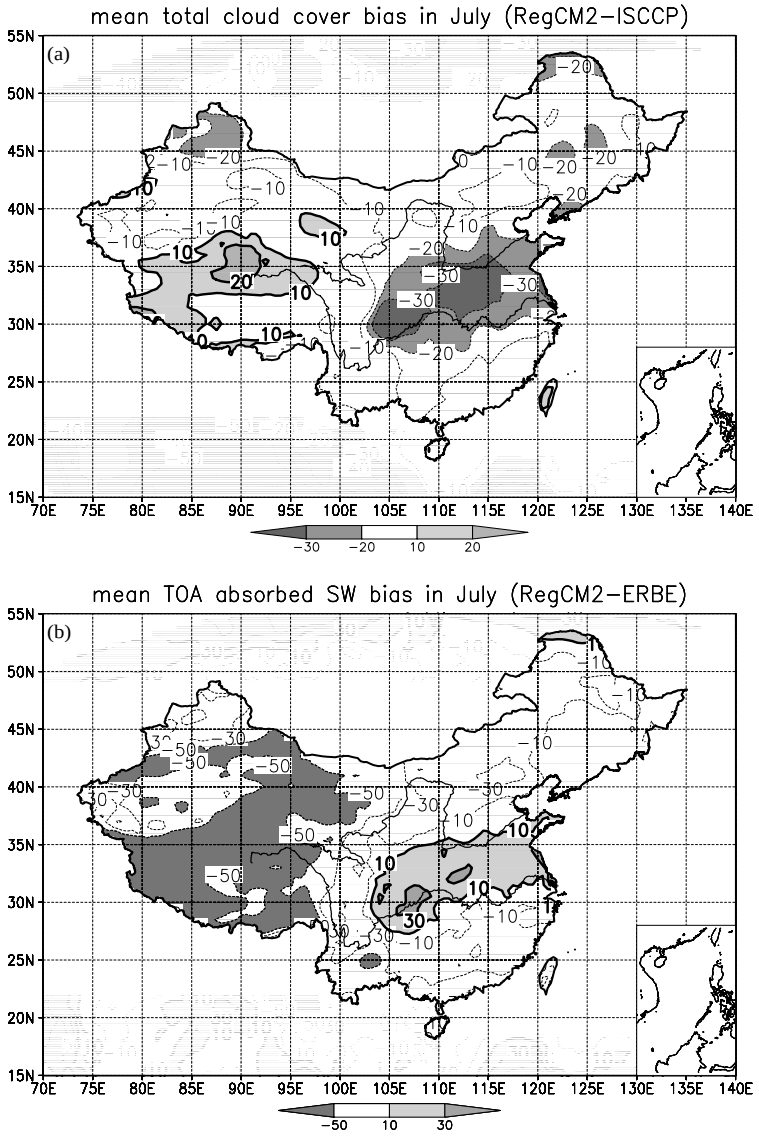

Fig. 8. Bias patterns of (a) mean total cloud cover (RegCM2-ISCCP) and (b) mean TOA absorbed SW (RegCM2-ERBE) in July. Unit: % for (a), W m^{-2} for (b).

reduces the TOA absorbed SW radiation bias over the Tibetan Plateau. Figure 9 shows the simulated TOA absorbed SW over the Tibetan Plateau before and after increasing the cloud droplet effective radius in the radiative parameterization scheme. The cloud droplet effective radius, to a certain extent, is also responsible for this systematic bias. Therefore, it is very important to improve the algorithm of the cloud droplet effective radius in the cloud-radiative parameterization scheme for obtaining reasonable simulation results.

The systematic error in simulated total cloud cover possibly exerts an apparent effect on the precipitation field. Fig. 10 presents the simulated variation of the total cloud cover bias in East China (110°–120°E) with season. It is very evident that the negative bias center of simulated cloud cover seasonally moves along with the seasonal rain belt. The negative bias center lies to the south of 27°N from January to March, jumps to around 33°N in July, then gradually retreats southward in September. As illustrated previously, the major seasonal rain belt displays two distinct northward jumps and three stationary periods in East Asia. It is located in South China before the first decade of June; then it abruptly jumps northward to the Yangtze River-Huaihe River Basins in the second decade of June, with these areas entering mei-yu periods; and the second northward jump occurs in mid July when North China starts its rainy season. These character-

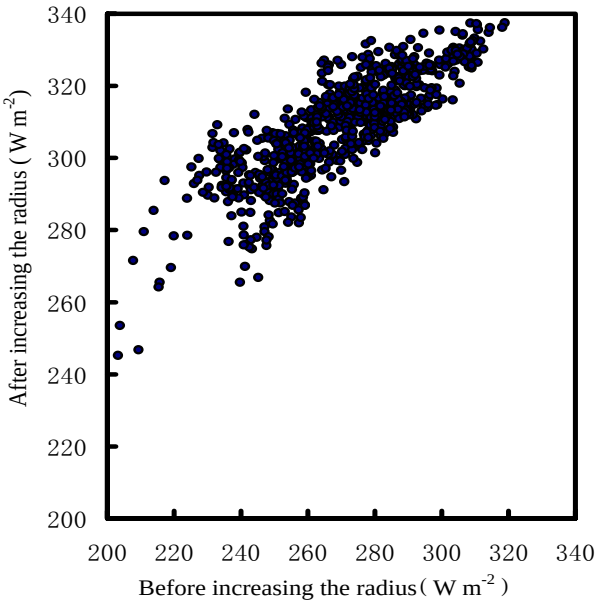

Fig. 9. Scatter diagram showing the simulated TOA absorbed SW over the Tibetan Plateau in July 1997, before and after increase of cloud drop effective radius in the radiative transfer parameterization scheme. Unit: W m^{-2}.

istics are clearly reflected in the observations (Fig. 10c). Although the simulation generally shows a seasonal march of the seasonal rain belt, one can find many significant biases when comparing it to the observations (Fig. 10b). For example, the rainfall amount is obviously underestimated in the pre-summer rainy season in South China, which is associated with too little simulated cloud cover; the mei-yu period is much shorter due to the negative bias of clouds in the Yangtze River-Huaihe River Basins; the simulated cloudiness is greater in North and Northeast China from mid summer to mid autumn, thus leading to a longer rainy season there, and the late southward retreat of the seasonal rain belt, until late September. The time of the second northward jump is earlier, which corresponds to more clouds being simulated in North China.

The vertical resolution of the model can affect the radiation flux and other variables. Figure 11 shows the vertical distribution of cloud amount for different vertical resolutions of 14, 17 and 20 levels. It can be seen that there is no obvious change in cloud vertical structure when the resolutions are 14 and 17 levels, whereas cloud is thinner and changes from mid-high cloud to high cloud when the model has a finer vertical resolution of 20 levels. Naturally, the change of cloud vertical structure will affect the radiation redistribution, thus changing the atmospheric temperature profile and surface temperature. Figure 12 indicates the simulated zonally averaged surface air temperature corresponding to the different vertical resolutions

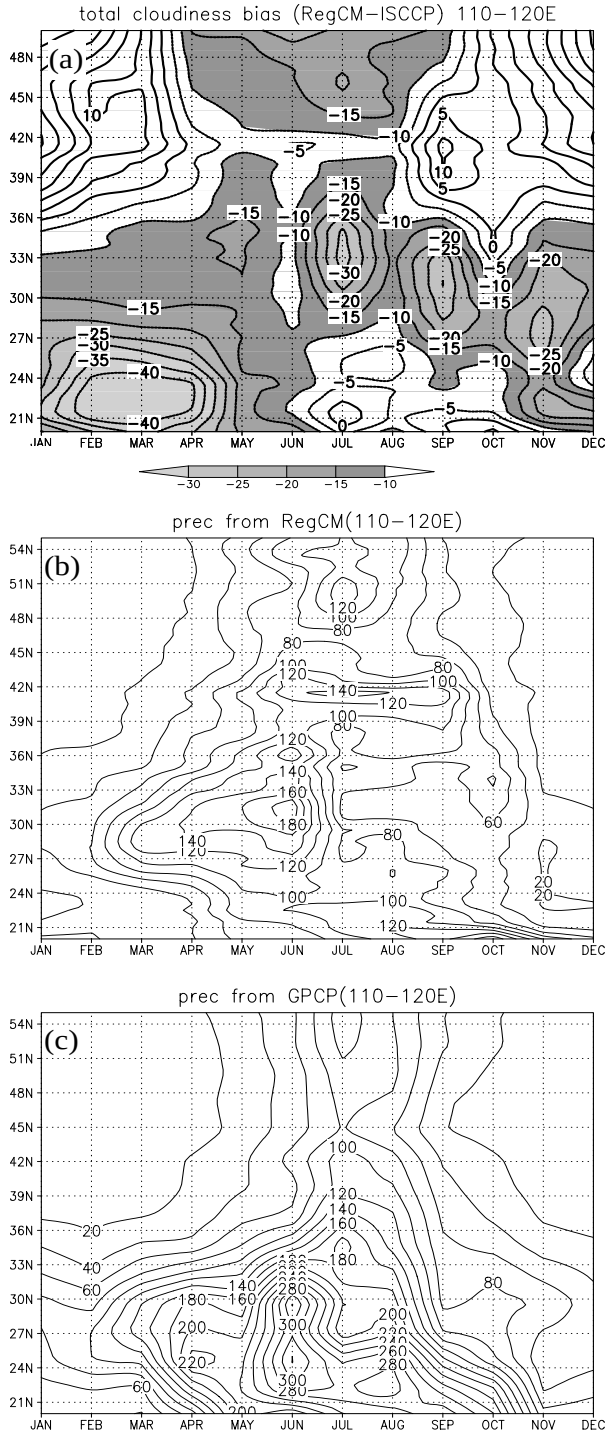

Fig. 10. (a) The 5-yr simulated biases of the total cloud amount, (b) the seasonal march of the major seasonal rain belt in East China (110°–120°E), and (c) the observed seasonal march of the major reasonable rain belt produced by the GPCP dataset. Unit: mm.

as shown in Fig. 11. It is apparent that the simulated surface temperature with a vertical resolution of 20

Table 2. Simulated net TOA radiation budget. (Unit: W m^{-2}).

	Jan.	Feb.	Mar.	Apr.	May.	Jun.	Jul.	Aug.	Sep.	Oct.	Nov.	Dec.	Average
Budget	−3.08	−2.99	−8.94	−5.67	−1.13	−5.14	−3.00	−16.63	−6.67	−8.70	−3.5	−0.52	−5.65

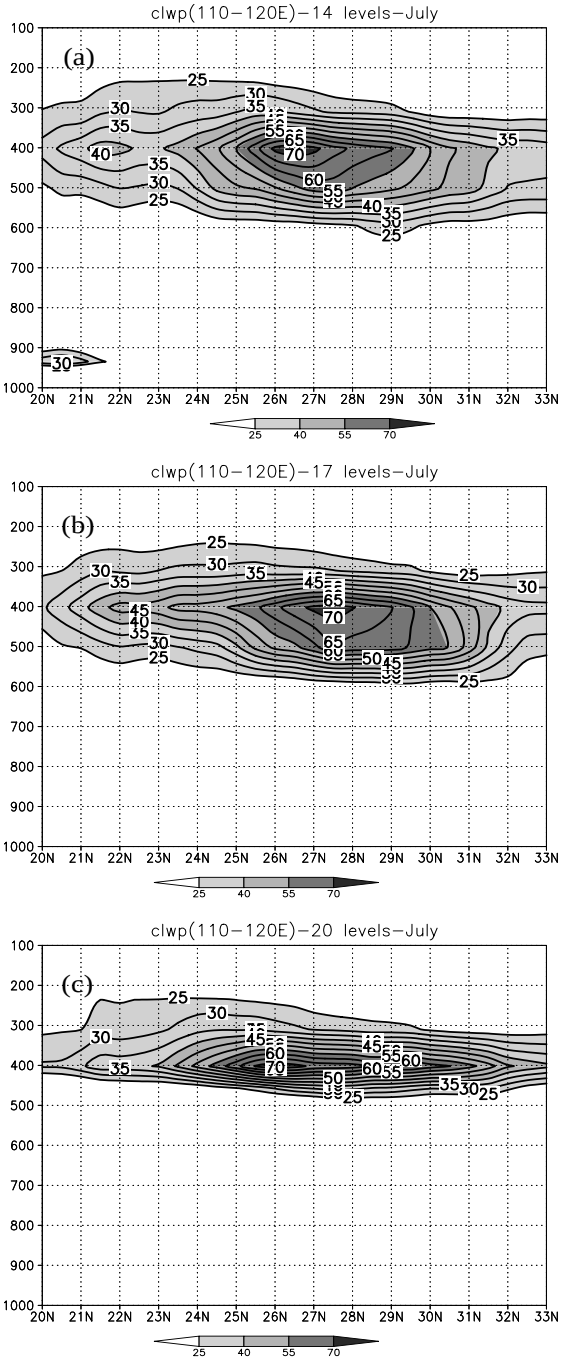

Fig. 11. Vertical distribution of cloud amount for different model vertical resolutions for July 1997. (a) 14 levels in the vertical, (b) 17 levels, and (c) 20 levels. Unit: g m^{-2}.

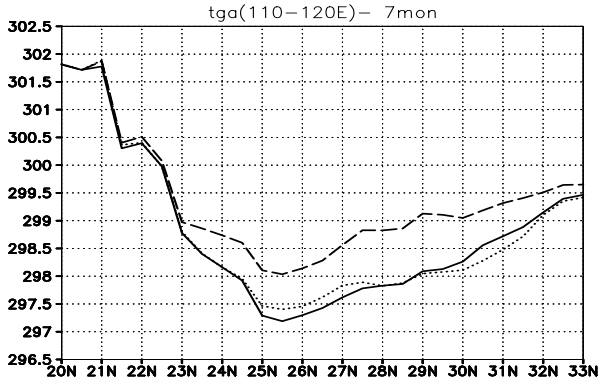

Fig. 12. The sensitivity of the simulated surface temperature in July 1997 in East China (110°–120°E) to the vertical division of the model. The dashed line is 20 levels; the dotted line is 17 levels; and the bold line is 14 levels. Unit: K.

levels is higher than those of the 14 and 17 levels, even 1 K higher than the value of the control experiment with 14 levels. This is owing to the fact that low clouds have a great reflectivity while high clouds have a great greenhouse effect to warm the atmosphere.

6. Boundary layer processes and the treatment of large-scale topography

6.1 *Boundary layer process*

As illustrated in the introduction, the diurnal variations of precipitation, temperature and wind in regional climate models have not yet been well reproduced. One reason for this deficiency may be attributed to unrealistic simulations of the boundary layer process in the RegCM2. Figure 13 shows the vertical profiles of biases of the simulated atmospheric temperature in the RegCM2 by using the Holtslag scheme (solid line). The observed data used are the NCEP/NCAR reanalysis data. It can be seen that temperature departures in the middle and high troposphere are generally small, whereas departures in the boundary layer below 850 hPa are very significant for the four different types of vegetation conditions. This implies that the vertical distributions of air temperature in the lower troposphere are not well reproduced, due possibly to the parameterization schemes of boundary layer processes. This effect is also true for other variables such as specific humidity, height and precipitation.

In order to improve simulations in the lower tropo-

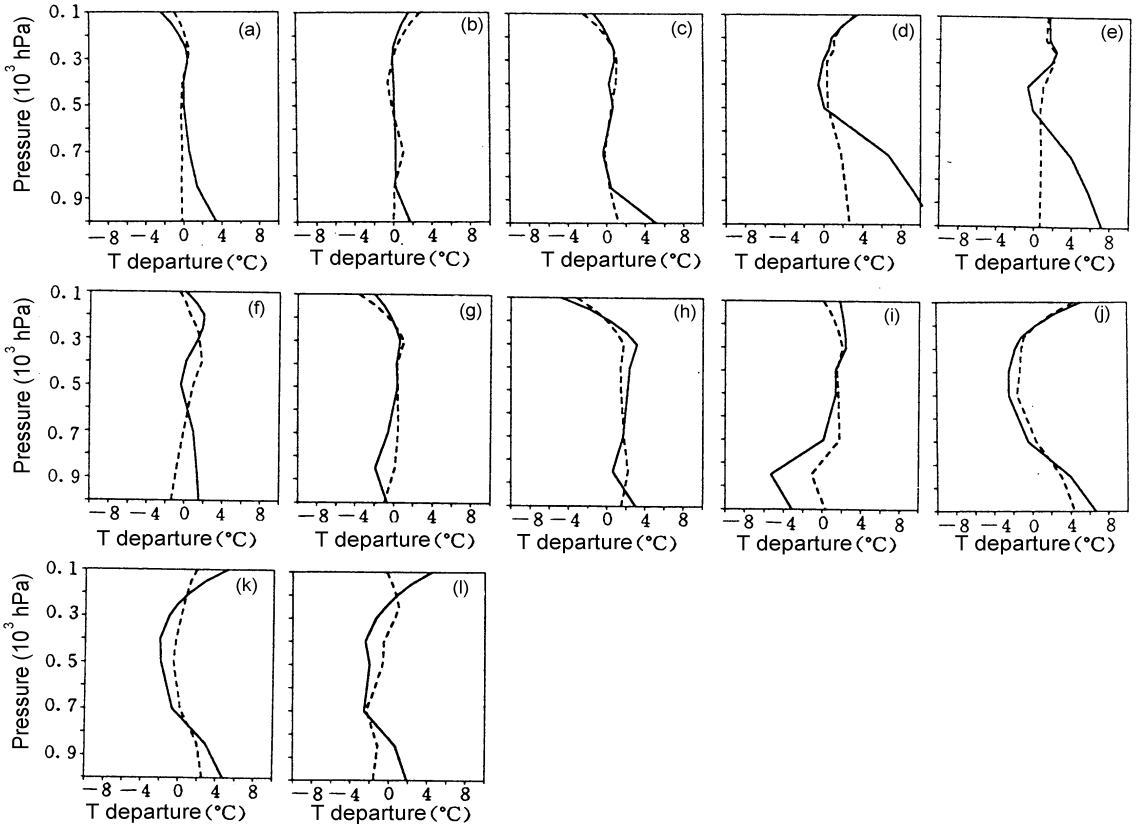

Fig. 13. The mean vertical profiles of simulated temperature biases for the 1991 summer (June, July and August) for four underlying surfaces: (a)–(c) grassland, (d)–(f) Plateau area, (g)–(i) agricultural land and (j)–(k) deserts. Solid lines denote departures or biases of the simulation made by using the Holtslag scheme and the dashed lines the biases of the simulation made by using the TKE scheme. Unit: °C (Zheng et al., 1999).

sphere in the RegCM2, one important step is to improve boundary layer parameterization schemes in the RegCM2. Here, the turbulent kinetic energy (TKE) closure scheme is used to treat the boundary layer processes (Yamada and Mellor, 1975; Theory and Lacarrere, 1983). In the RegCM2, either the bulk boundary layer or high-resolution parameterization schemes treats the height of the boundary layer and the eddy diffusion coefficient K in a relatively simple way. The TKE scheme can improve the computational accuracy of the K coefficient in the K-theory and more realistically simulate the process of diurnal variations by taking into account the continuous interactive adjustment between the mean field and turbulent field. Figure 14 is the mean diurnal variations of heights of the boundary layer for five underlying surface conditions for summer 1991. The diurnal variation of the boundary layer height simulated by the RegCM2 with the inclusion of the Holtslag scheme is very weak while that simulated by the RegCM2 with the inclusion of the TKE scheme is quite marked. The local maximum occurs in early afternoon, with heights extending upward to 1–1.8 km. The Tibetan Plateau has the highest height of the boundary layer (1.8 km), which is consistent with the observed heights of 2.0–2.1 m measured in the Tibetan Plateau Experiment (TIPEX) in summer 1979 (Miao et al., 1998). The occurrence timing of local maximum heights for the desert and the plateau areas is 2 hours later than the grassland and the agricultural regions. The boundary layer height for the oceanic area shows a weak diurnal variation due to a small difference of daytime and nighttime heating. In addition, from Fig. 13, it can be seen that the biases simulated with use of the TKE scheme are generally much reduced in the middle and lower troposphere, implying that the effect of the boundary layer processes is significantly improved, especially for the highland region (Figs. 13d–f). In fact, the large-scale circulation and precipitation fields have also been improved to a varying degree.

6.2 *Improved treatment of large-scale topographical effects*

As depicted in Fig. 1, the domain under study in-

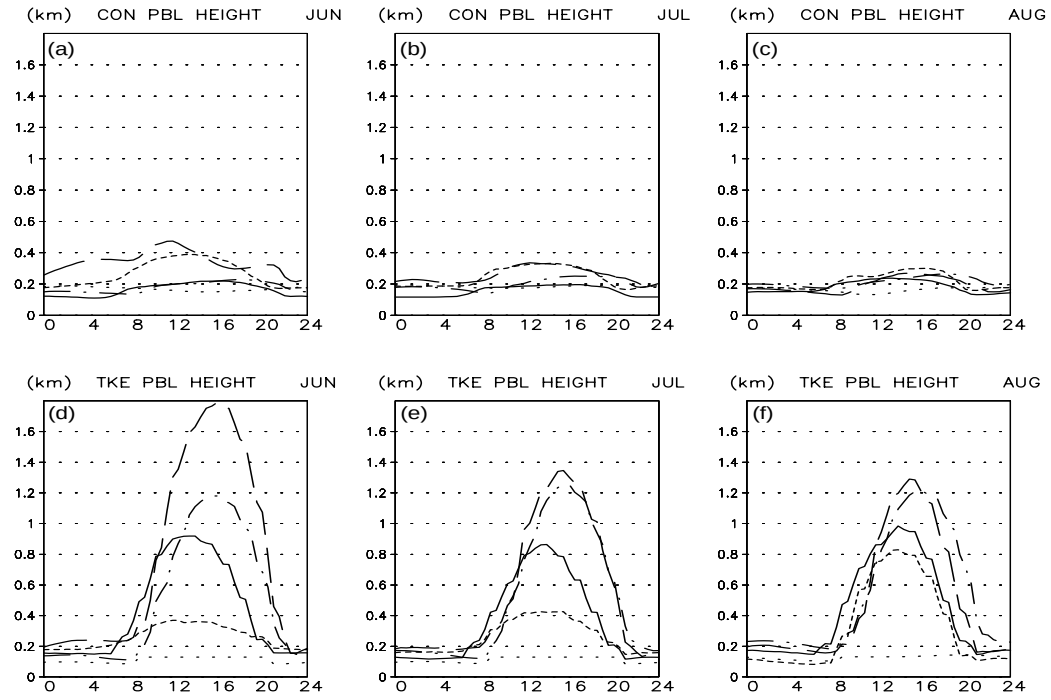

Fig. 14. Simulated diurnal cycle of boundary layer heights for different underlying surfaces in the 1991 summer (June, July and August). (a)–(c) for the simulated curves by using the Holtslag scheme and (d)–(f) for the simulated curves by using the TKE scheme. Solid line: grassland; long dashed line: highlands; short dashed: crops; dotted line: ocean; and dotted dashed line: deserts (Zheng et al., 1999).

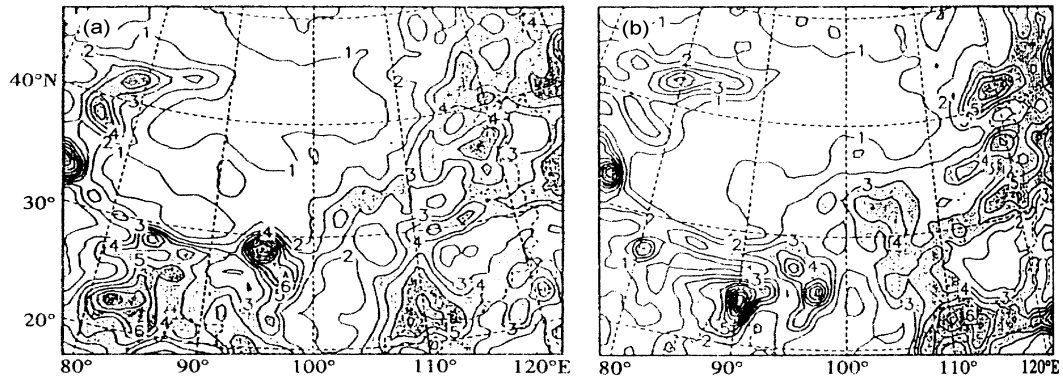

Fig. 15. Distributions of monthly rainfalls in China for June 1991 simulated (a) by the RegCM2 without use of the error subtraction method for computing horizontal pressure gradient force, and (b) by the RegCM2 with use of the error subtraction method (Qian, 1999).

cludes the huge Tibetan Plateau which has a very steep slope in the eastern and southern foothills. In addition, there are many multi-scale mountain peaks and valleys. The existence of these complex terrain features may cause computational instability around the Tibetan Plateau, thus leading to an unstable condition and unrealistic results. This kind of instability results from great errors in computing the horizontal pressure gradient force over steep sloping areas. Therefore, how to retain the realistic topography in the RegCM2 as much as possible, and at the same time eliminating or reducing computational instability and the spurious precipitation centers near the Tibetan Plateau resulting from the steep topography, is one of the important issues in simulating and predicting the East Asian climate by using the RegCM2.

The error subtraction method was used to improve the computational accuracy (Zheng and Qian, 1999;

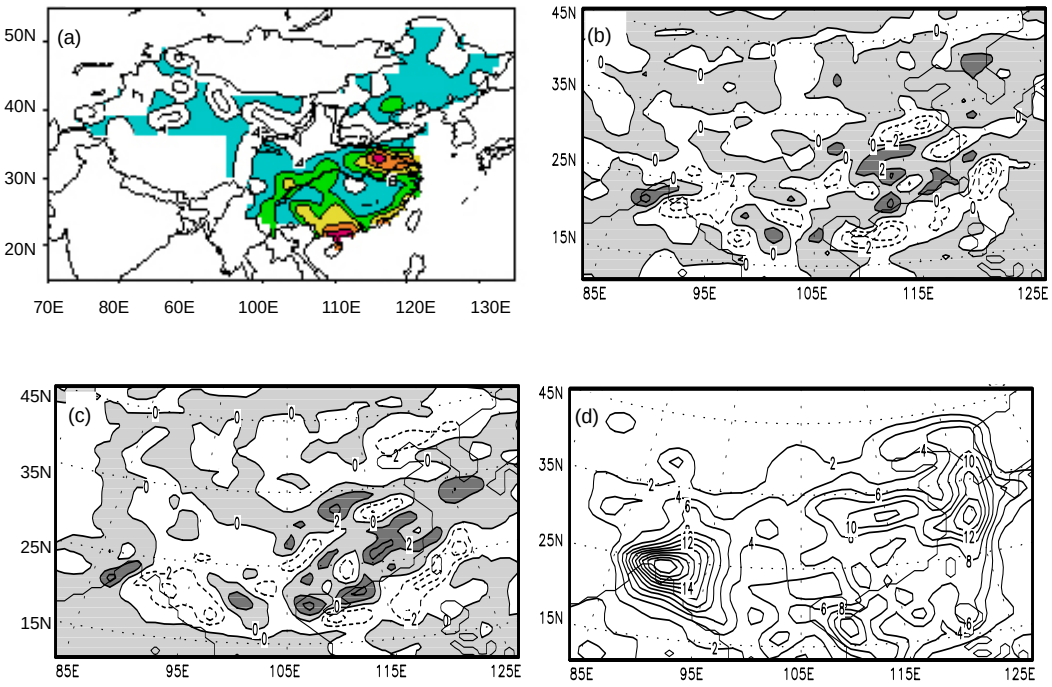

Fig. 16. (a) The observed precipitation pattern in June 1991. (b) The precipitation difference pattern between the precipitation field simulated with introduction of an envelope orography and RegCM2. (c) The precipitation difference pattern between the precipitation field simulated with the effect of gravity wave drag and RegCM2. (d) The simulated precipitation patterns by using RegCM2. Unit: mm d^{-1}. (Liu and Qian, 2001).

Qian et al., 1999). Here, we will not discuss the details of this method, only showing the simulated results from using it. The observed precipitation in June 1991 is given in Fig. 16a. It can be clearly seen that a large area of spurious precipitation simulated by the RegCM2 for June 1991 is located to the southeast of the Tibetan Plateau where there is very steepy topography, although the major seasonal rain belt along the Yangtze River-Huaihe River basins was well reproduced (Fig. 15a). The simulated rainfall pattern by using the error subtraction method in the RegCM2 indicated a significant improvement, with the spurious heavy precipitation area nearly eliminated (Fig. 15b). Improvements of the precipitation simulations were seen in other regions such as North China, the Yangtze River-Huaihe River basin and the Bay of Bengal.

Besides the spurious heavy precipitation near steep slopes of the large-scale terrain features, systematic errors or biases in climate simulations and predictions may be also caused by inadequate description of effects of small scale topography in the models. The method to address the climate effect of small-scale terrain features is the use of subgrid-scale orographic parameterization schemes (Qian, 2000; Liu and Qian, 2001; Leung and Ghan, 1998). One of the methods is the introduction of an envelope orography. Another method is the consideration of the effect of gravity wave drag excited by small scale topography in the RegCM2 which possibly improves the simulation of the horizontal wind field (McFarlane, 1987). Based on our tests of these two methods (Fig. 16), the improvement of simulations of monthly precipitation was significant, especially for the inclusion of the effect of gravity wave drag. One may clearly see the spurious heavy precipitation center near the southeastern sloping region of the Tibetan Plateau (Fig. 16d). Major improvements are the increase of precipitation in Southeast China and the middle and lower Yangtze River basin (Figs. 16b, c). However, these two subgrid scale orographic effects were insignificant in the initial integration and then their effects were enhanced as the integration time increased. For climate simulations with long integration, the introduction of an envelope orography and inclusion of the effect of gravity wave drag can improve the simulation results, especially for the precipitation, temperature and wind fields.

7. Summary and conclusions

In this paper, a sensitivity study on the main physical parameterization schemes used in the RegCM2

has been described in connection with climate simulations of seasonal rain belts and the 1991, 1994 and 1998 extreme flooding events in China. Four physical processes have been studied that significantly affect the simulation results in the model through a comparative testing experiment: the land surface process, convective precipitation, cloud-radiation transfer process, and boundary layer process and large-scale topography. Among them, the most sensitive physical processes for the precipitation simulations are believed to be the cloud-radiation transfer processes and convective precipitation representation. These two processes are not independent from each other. The total cloud amount and their vertical distribution greatly depend on the cumulus parameterization scheme. On the other hand, the convective precipitation is considerably affected by the cloud-radiation transfer process through the feedback mechanism by changing the atmospheric heating fields, surface fluxes and atmospheric stability. In the East Asia monsoon region, the cloud type and vertical configurations have prominent features. The observations indicate that major seasonal cloud bands such as the mei-yu/Baiu are usually characterized by elongated low and mid-level cloud bands with a number of convective cloud clusters or meso-scale cloud systems embedded within it (Niniomiya and Murakami, 1987). Therefore, a more realistic cloud parameterization scheme suitable for representing the interaction of this mixed type of cloud is desirable.

The precipitation episodes in an extreme flooding event in East Asia are significantly modulated by intraseasonal oscillations with the peak period ranging from 20 days to 90 days, mostly 20–30 days and 40–60 days (Wang and Xu, 1997). The occurrence of propagation of the intraseasonal oscillation (ISO) is associated with the cloud-precipitation and surface processes feedback mechanism. Therefore, the cloud parameterization and radiative transfer schemes not only play a crucial role in the simulation of rainfall amounts, patterns and intensity, but also are fundamental for simulations of repeated occurrence of rain episodes under the modulation of the ISO.

The parameterization schemes of the land surface processes may exert an important effect on the precipitation and surface temperature in pattern and magnitude. The surface temperature is very sensitive to the surface process parameterization schemes. Our experiments have shown that a finer vertical resolution of the soil layer, especially in the plant root zone (0.5–2 m), is necessary for improved climate simulation. In the East Asian region, the inclusion of the Tibetan Plateau in regional climate models is indispensable for a realistic simulation of the East Asian monsoon activity and the seasonal rain belt. However, in doing so, extensive areas of the apparent spurious heavy precipitation over the steep sloping regions usually occur in the model. They can be mostly eliminated with adequate methods, such as the introduction of an envelope orography and inclusion of the effect of gravity wave drag. Therefore, the thermal and dynamic effects of the Tibetan Plateau can be well represented in an expanded domain of the model. For better simulations of diurnal variations and vertical distributions of meteorological variables in the middle and lower troposphere, an improved representation of the boundary layer process is also very important.

Based on our sensitivity experiments for the above four key physical processes in the RegCM2, we have found that the MFS and Betts-Miller scheme (BM) for convective precipitation are more suitable for the simulations of precipitation in the East Asia region. The radiation transfer scheme used in CCM3 GCM may be used in the regional climate modeling, but with a rather systematic error and uncertainty. A further improvement needs to be done in the future. The modified land surface process models of the BATS type (LPMI and LPMII) show a better performance in the East Asian regional simulations. They will be used in the RegCM2 together with the original BATS. Likewise, the TKE scheme for boundary layer processes will be used in the RegCM2 as an additional option. Due to the use of a larger domain including the entire Tibetan Plateau, the treatment schemes of large-scale terrain features will be included in the RegCM2. Incorporating all the above modifications and new additional options into the RegCM2, a modified version of the RegCM2 has been developed with which a ten-year regional model climatology and hindcasts in China have been made. They will be reported upon in the second part of the present paper.

Acknowledgments. The authors would like to thank NCAR for providing the NCEP/NCAR reanalysis data. This work was supported by the Assessments of Impacts and Adaptations to Climate Change in Multiple Regions and Sectors (AIACC) AS25 project, the State Key Project of Research and Development of the Short-term Climate Prediction Systems (Grant No. 96–908) and SCSMEX project.

REFERENCES

Anthes, R. A., 1977: A cumulus parameterization scheme utilizing a one-dimensional cloud model. *Mon. Wea. Rev.,* **105**, 270–286.

Anthes, R. A., E. Y. Hsie, Y. H. Kuo, 1987: Description of the Penn State/NCAR Mesoscale Model Version 4 (MM4). Tech. Note NCAR/TN-282+STR, 66pp.

Barkstrom, B. R., 1984: The earth radiation budget experiment (ERBE). *Bull. Amer. Meteor. Soc.*, **65**, 1170–1185.

Betts, A. K., and M. J. Miller, 1986: A new convective adjustment scheme. Part 2: Single column tests using GATE wave, BOMEX, ATEX and arctic air-mass datasets. *Quart. J. Roy. Meteor. Soc.*, **112**, 693–709.

Chan, Johnny C. L., Y. Liu, K. C. Chow, Y. Ding, William K.M. Lau, and K. L. Chan, 2004: Design of a regional climate model for the simulation of South China summer monsoon rainfall. *J. Meteor. Soc. Japan,* **82**, 1645–1665.

Chen Bomin, 1996: Forecast experiments of modified ECMWF mass flux cumulus parameterization scheme. *Plateau Meteorology*, **15**, 37–47. (in Chinese)

Dickinson, R. E., A. Henderson-Sellers, P. J. Kennedy, 1993: Biosphere-Atmosphere Transfer Scheme (BATS) Version 1e as coupled to the NCAR Community Climate Model. NCAR/ TN-387+STR, 72pp.

Ding Yihui, 1993: *Research on the 1991 Persistent, Severe Flood over Yangtze-Huaihe River valley.* Chinese Meteorological Press, 255pp. (in Chinese)

Ding Yihui, 1994: *Monsoons over China.* Kluwer Academic Publishers, 419pp.

Ding Yihui, and Liu Yanju, 2001: Onset and the evolution of the summer monsoon over the South China Sea during SCSMEX field experiment in 1998. *J. Meteor. Soc. Japan*, **79**, 255–276.

Ding Yihui, Zhang Jing, and Zhao Zongci, 1998: An improved land-surface processes model and its simulation experiment. Part II: An improved land surface processes model and its simulation experiment. Part II:land processes model (LPM–ZD) and its coupled simulation experiment with regional climate model. *Acta Meteorologica Sinica*, **56**, 385–400. (in Chinese)

Ding Yihui, and Coauthors, 2000: Improvement of high-resoulution regional climate model and its application to numerical simulation of prolonged heavy rainfalls in East Asia. *Development of Operational Short-term Climate Model, Series 2.* Ding Yihui, Ed., China Meteorological Press, Beijing, 217–231. (in Chinese)

Ding Yihui, Liu Yiming, Song Yongjia, and Li Qingquan, 2002: Research and experiments of the short-term climate dynamical prediction model system in China. *Climatic and Environmental Research*, **7**, 236–246. (in Chinese)

Ding Yihui, and Coauthors, 2004a: Advance in seasonal dynamical prediction operation in China. *Acta Meteorologica Sinica,* **62**, 598–612. (in Chinese)

Ding Yihui, Shi Xueli, Sun Ying, and Liu Yiming, 2004b: Simulations and predictions for flooding season in China by using the nested regional climate model. *Chinese Journal of Atmospheric Sciences*, **28**, 205–217.

Gates, W. L., and Coauthors, 1999: An overview of the results of the Atmospheric Model Intercomparison Project (AMIP 1). *Bull. Amer. Meteor. Soc.*, **80**, 29–55.

Giorgi, F., M. R. Marinucci, G. De Canio, and G. T. Bates, 1993a: Development of a second-generation regional climate model (RegCM2), Part I: Boundary layer and radiative transfer processes. *Mon. Wea. Rev.*, **121**, 2794–2813.

Giorgi, F., M. R. Marinucci, and G. T. Bates, 1993b: Development of a second-generation regional climate model (RegCM2). Part II: Convective processes and assimilation of lateral boundary conditions. *Mon. Wea. Rev.*, **121**, 2814–2832.

Giorgi, F., L. O. Mearns, C. Shield, and L. Meyer, 1996: A regional model study of the importance of local versus remote controls of the 1988 drought and the 1993 flood over the central United States. *J. Climate*, **9**, 1150–1162.

Giorgi, F., and C. Shields, 1999: Tests of precipitation parameterizations available in the latest version of the NCAR regional climate model (RegCM) over the continental U.S. *J. Geophys, Res.*, **104**, 6353–6376.

Giorgi, F., and L. O. Mearns, 1999: Introduction to special section: Regional climate modeling revisited. *J. Geophys. Res.*, **104**, 6335–6352.

Giorgi, F., Y. Huang, K. Nishizawa, and C. Fu, 1999: A seasonal cycle simulation over eastern Asia and its sensitivity to relative transfer and surface processes. *J. Geophys. Res.*, **104**, 6403–6423.

Giorgi, F., and B. Hewitson, 2001: Regional climate information—Evaluation and projection. *Climate Change 2001: The Scientific Basis.* Houghton et al., Eds., Cambridge University Press, Cambridge, UK, 585–638.

Grell, G. A., 1993: Prognostic evaluation of assumptions used by cumulus parameterizations, *Mon. Wea. Rev.*, **121**, 764–787.

Holtslag, A. A. M., E. I. F. De Bruijn, and H.-L. Pan 1990: A high-resolution air-mass transformation model for short-range weather forecasting. *Mon. Wea. Rev.*, **118,** 1561–1575.

Hong, S.-Y., H.-M. H. Juang, and D.-K. Lee, 1999: Evaluation of a regional spectral model for the East Asian monsoon case studies for July 1987 and 1988. *J. Meteor. Soc. Japan*, **77**, 553–572.

Kang, I.-S., and Coauthors, 2002: Intercomparsion of the climatological variations of Asian summer monsoon precipitation simulated by 10 GCMs. *Climate Dyn.*, **19**, 383–395.

Kiehl, J. T., J. Hack, G. Bonan, B. Boville, B. Briegleb, D. Williamson, and P. Rasch, 1996: Description of the NCAR Community Climate Model (CCM3). NCAR Tech. Rep., TN-420+STR, 152pp.

Lee, D.-K., and M.-S. Suh, 2000: Ten year Asian summer monsoon simulation using a regional climate model (RegCM2). *J. Geophys. Res.*, **105**, 29565–29577.

Leung, L. R., and S. J. Ghan, 1998: Parameterization subgrid orographic precipitation and surface cover in climate models. *Mon. Wea. Rev.*, **126**, 3271–3291.

Leung, L. R., S. J. Ghan, Z. C. Zhao, Y. Luo, W.-C. Wang, and H. L. Wei, 1999: Inter-comparison of regional climate simulations of 1991 summer monsoon in eastern Asia. *J. Geophys. Res.,* **104**, 6425–6454.

Liu Huaqiang, and Qian Yongfu, 2001: Effects of envelope orograpy and gravity wave drag parameterization on regional climate simulation. *Chinese Journal of Atmospheric Sciences*, **25**, 209–220.

Liu Huaqiang, Qian Yongfu, and Zheng Yiqun, 2002: Effects of nested area size upon regional climate model simulations. *Adv. Atmos. Sci.*, **19**, 111–120.

Liu Yiming, and Ding Yihui, 2002a: Modified mass flux cumulus convective parameterization scheme and its simulation experiment—Part I: Mass flux scheme and its simulation of the 1991 flood event. *Acta Meteorologica Sinica*, **16**, 37–49.

Liu Yiming, and Ding Yihui, 2002b: Simulation of heavy rainfall in the summer of 1998 over China with regional climate model. *Acta Meteorologica Sinica*, **16**, 346–362.

Liu, Y. Q., F. Giorgi, and W. M. Washington, 1994: Simulation of summer monsoon climate over East Asia with an NCAR regional climate model. *Mon. Wea. Rev.*, **122**, 2331–2348.

Liu, Y. Q., R. Avissar, and F. Giorgi, 1996: Simulation with the regional climate model RegCM2 of extremely anomalous precipitation during the 1991 East Asian flood: An evaluation study. *J. Geophys. Res.*, **101**, 26199–26215.

Luo Yong, Zhao Zongci, and Ding Yihui, 2002: Ability of NCAR RegCM2 in reproducing the dominant physical processes during the anomalous rainfall episodes in the summer of 1991 over the Yangtze-Huaihe valley. *Adv. Atmos. Sci.*, **19**, 236–254.

McFarlane, N. A., 1987: The effect of orographically excited gravity wave drag on the general circulation of the stratosphere and troposphere. *J. Atmos. Sci.*, **44**, 1175–1800.

Miao Manqian, Cao Hong, and Ji Jinjun, 1998: Analysis of turbulent characteristics in atmospheric boundary layer over the Qinghai-Xizang Plateau. *Plateau Meteorology*, **17**, 356–363. (in Chinese)

National Climate Center of China, 1998: *The 1998 Severe Flood and the Climate Anomaly*. China Meteorological Press, 139 pp. (in Chinese)

Ninomiya, K., and T. Murakami, 1987: The early summer rainy season (Baiu) over Japan. *Monsoon Meteorology*, C. P. Chang and T.N. Krishnmurti, Eds., Oxford University Press, 93–21.

Pan, Z., M. Segal, R. Turner, and E. Takle, 1995: Model simulation of impacts of transient surface wetness on summer rainfall in the United States Midwest during drought and flood years. *Mon. Wea. Rev.*, **123**, 1575–1581.

Pan, Z., E. Takle, W. Gutowski, and R. Turner, 1999: Long simulation of regional climate as a sequence of short segments. *Mon. Wea. Rev.*, **127**, 308–321.

Qian Yongfu, 2000: Effects of envelope orography and gravity wave drag on performance of climate modeling. *Quart. J. Appl. Meteor.*, **12**, 14–20. (in Chinese)

Qian Yongfu, Wang Qianqian, Liu Huaqiang, and Zheng Weizhong, 1999: Numerical modelings and problems of regional climate changes in China. *Plateau Meteorology*, **18**, 341–349. (in Chinese)

Rossow, W. B., and R. A. Schiffer, 1991: ISCCP cloud data products. *Bull. Amer. Meteor. Soc.*, **72**, 2–20.

Small, E. E., F. Giorgi, and L. C. Sloan, 1999: Regional climate model simulation of precipitation in central Asia: Mean and interannual variability. *J. Geophys. Res.*, **104**, 6563–6582.

Sperber, K. R., and Coauthors, 2001: Dynamic seasonal predictability of the Asian summer monsoon. *Mon. Wea. Rev.*, **129**, 2226–2248.

Therry, G., and P. Lacarrere, 1983: Improving the eddy kinetic energy model for planetary boundary layer description. *Bound.-Layer Meteor.*, **25**, 63–88.

Tiedtke, M., 1989: A comprehensive mass flux scheme for cumulus parameterization in large-scale schemes. *Mon. Wea. Rev.*, **117**, 1179–1800.

Wang, B., and X. H. Xu, 1997: Northern Hemisphere summer monsoon singularities and climatological intraseasonal oscillation. *J. Climate*, **10**, 1071–1085.

Wang, W.-C., W. Gong, and H. L. Wei, 2000: A regional model simulation of the 1991 severe precipitation event over the Yangtze-Huai River Valley. Part I: Precipitation and circulation statistics. *J. Climate*, **13**, 74–92.

Wang, Y. Q., O. L. Sen, and B. Wang, 2003: A higher resolved regional climate model (IPRC-RegCM) and its simulation of the 1998 severe precipitation event in China. Part I: Model description and verification of simulation. *J. Climate*, **16**, 1721–1738.

Wang, Y. Q., L. R. Leung, J. L. McGregor, D. K. Lee, W.-C. Wang, Y. Ding, and F. Kimura, 2004: Regional climate modeling: Progress, challenges, and prospects. *J. Meteor. Soc. Japan*, **82,** 1599–1628.

Yamada, T., and G. Mellor, 1975: A simulation of the Wangara atmospheric boundary layer data. *J. Atmos. Sci.*, **32**, 2309–2329.

Zhai Guoqing, Gao Kun, and J. S. Pan, 2003: The sensitivity experiments of Betts-Miller convective parameterization scheme in regional climate simulation. *Chinese J. Atmos. Sci.*, **27**, 330–344. (in Chinese)

Zhang Jing, and Ding Yihui, 1998: An improved land-surface processes model and its simulation experiment. Part I: Land-surface processes model (LPM-ZD) and its off-line tests and performance analysis. *Acta Meteorologica Sinica*, **56**, 2–19. (in Chinese)

Zhang Xiuzhi, Wu Xunying, and He Jinhai, 2004: Vertical character of soil moisture in China. *Acta Meteorologica Sinica*, **62**, 51–61. (in Chinese)

Zheng Yiqun, Miao Manqian, and Qian Yongfu, 1999: Turbulence kinetic energy turbulence closure scheme applied to regional climate modeling. *Acta Meteorologica Sinica*, **57**, 641–650. (in Chinese)

Zheng Yiqun, Qian Yongfu, Q. J. Gui, and G. Yu, 2002: Effects of initial/lateral boundary conditions on regional climate simulations. *Chinese J. Atmos. Sci.*, **26**, 794–806. (in Chinese)

Zheng Weizhong, and Qian Yongfu, 1999: Improvement on computing the horizontal pressure gradient force in the RegCM2. *Acta Meteorologica Sinica*, **13**, 304–315. (in Chinese)